

Hydrolytic cleavage of both CS₂ carbon-sulfur bonds by multinuclear Pd(II) complexes at room temperature

Xuan-Feng Jiang^{1,2}, Hui Huang^{2*}, Yun-Feng Chai³, Tracy Lynn Lohr⁴, Shu-Yan Yu^{1*}, Wenzhen Lai^{5*}, Yuan-Jiang Pan^{3*}, Massimiliano Delferro^{4*†} and Tobin J. Marks^{4*}

Developing homogeneous catalysts that convert CS₂ and COS pollutants into environmentally benign products is important for both fundamental catalytic research and applied environmental science. Here we report a series of air-stable dimeric Pd complexes that mediate the facile hydrolytic cleavage of both CS₂ carbon-sulfur bonds at 25 °C to produce CO₂ and trimeric Pd complexes. Oxidation of the trimeric complexes with HNO₃ regenerates the dimeric starting complexes with the release of SO₂ and NO₂. Isotopic labelling confirms that the carbon and oxygen atoms of CO₂ originate from CS₂ and H₂O, respectively, and reaction intermediates were observed by gas-phase and electrospray ionization mass spectrometry, as well as by Fourier transform infrared spectroscopy. We also propose a plausible mechanistic scenario based on the experimentally observed intermediates. The mechanism involves intramolecular attack by a nucleophilic Pd-OH moiety on the carbon atom of coordinated μ-OCS₂, which on deprotonation cleaves one C-S bond and simultaneously forms a C-O bond. Coupled C-S cleavage and CO₂ release to yield [(bpy)₃Pd₃(μ₃-S)₂](NO₃)₂ (bpy, 2,2'-bipyridine) provides the thermodynamic driving force for the reaction.

The cleavage of carbon–sulfur (C–S) bonds by transition metals is of great interest from both fundamental catalytic and environmental standpoints^{1,2}. Hydrodesulfurization, the catalytic technology used to remove sulfur from hydrocarbons during refining, is one of the two most important steps in petroleum processing³. CS₂ and COS are major chemical feedstocks, particularly for cellophane and viscose rayon production^{4,5}, but when released into the environment form photochemical tropospheric sulfur aerosols^{6,7} to yield fog, haze and acid rain, which are harmful to human health and the environment^{8,9}. Conventional CS₂ abatement technologies, such as adsorption^{10,11}, thermal or catalytic combustion¹², and catalytic hydrolysis¹³ over supported metal oxides (Al, Ti, Zr and Nb) typically require high temperatures (>250 °C) (ref. 14) along with absorbent regeneration and challenging utilization of the dithiocarbamate products^{14–16}. Some microbial extremophiles can convert CS₂ into H₂S and CO₂ via the rapid cleavage of both C–S bonds under mild conditions (70–88 °C); however, the mechanistic details remain obscure and hence the active sites are difficult to simulate^{17,18}. At transition-metal centres, CS₂ is known to undergo a variety of reactions, including insertion, dimerization and disproportionation^{19–21}. Nevertheless, catalytic cleavage of both C–S bonds by a homogeneous transition-metal complex has, to the best of our knowledge, not been achieved. Cleaving the first C–S bond of CS₂ ($\Delta H_{\text{dissoc}} = 94.0 \text{ kcal mol}^{-1}$ for free CS₂)²² to produce L_nM(S) + L_nM(C–S) species (L_n, ancillary ligand array) has been reported²³; however, cleavage of the second C–S bond is rare^{24,25}, which presumably reflects, among other

factors, the very large bond-dissociation enthalpy of the remaining C–S bond (171.5 kcal mol⁻¹ for free CS)^{22,26}. For these reasons, well-understood approaches to efficient CS₂ desulfurization are highly desirable.

Results

Reaction of CS₂ with dimeric Pd complexes. Here we report a synthetic and mechanistic investigation of the hydrolytic desulfurization of CS₂ mediated by the air-stable dimeric Pd complexes, [(N⁺N)₂Pd₂(NO₃)₂](NO₃)₂ (N⁺N, 2,2'-bipyridine, 4,4'-dimethylbipyridine or 1,10-phenanthroline) at room temperature, to generate CO₂ and trinuclear [(N⁺N)₃Pd₃(μ₃-S)₂](NO₃)₂ clusters. Furthermore, the [(N⁺N)₂Pd₂(NO₃)₂](NO₃)₂ dimers are quantitatively regenerated by the addition of HNO₃ to yield a Pd-dimer-mediated aqueous cycle that converts CS₂ and HNO₃ into CO₂ + SO₂ + NO₂ (Fig. 1). Also, HNO₃ can be hydrolytically regenerated from NO₂ in the Oswald process for HNO₃ production²⁷, and the addition of Ba²⁺ and HNO₃ precipitates BaSO₄ to yield an overall cycle for CS₂ conversion into CO₂ and the environmentally benign BaSO₄. Although di- and polynuclear Pd complexes are known to react stoichiometrically with CS₂, which involves CS₂ insertion into, or coordination to, the Pd–Pd bond^{27–31}, the present results indicate that dinuclear metal complexes provide a platform for hydrolytic C–S bond cleavage that involves both C–S moieties and, ultimately, a promising strategy for neutralizing CS₂, COS and other toxic organosulfur compounds.

¹Beijing Key Laboratory for Green Catalysis and Separation, Laboratory for Self-Assembly Chemistry, Department of Chemistry and Chemical Industry, College of Environmental and Energy Engineering, Beijing University of Technology, Beijing 100124, China. ²College of Materials Science and Opto-electronic Technology and Key Laboratory of Vacuum Physics, University of Chinese Academy of Sciences, Beijing 100049, China. ³Department of Chemistry, Zhejiang University, Hangzhou 310027, China. ⁴Department of Chemistry and the Center for Surface Science and Catalysis, Northwestern University, Evanston, Illinois 60208, USA. ⁵Department of Chemistry, Renmin University of China, Beijing 100872, China. [†]Present address: Chemical Sciences and Engineering Division, Argonne National Laboratory, Lemont, Illinois 60439, USA. *e-mail: selvesassembly@bjut.edu.cn; huihuang@ucas.ac.cn; panyuanjiang@zju.edu.cn; delferro@anl.gov; t-marks@northwestern.edu

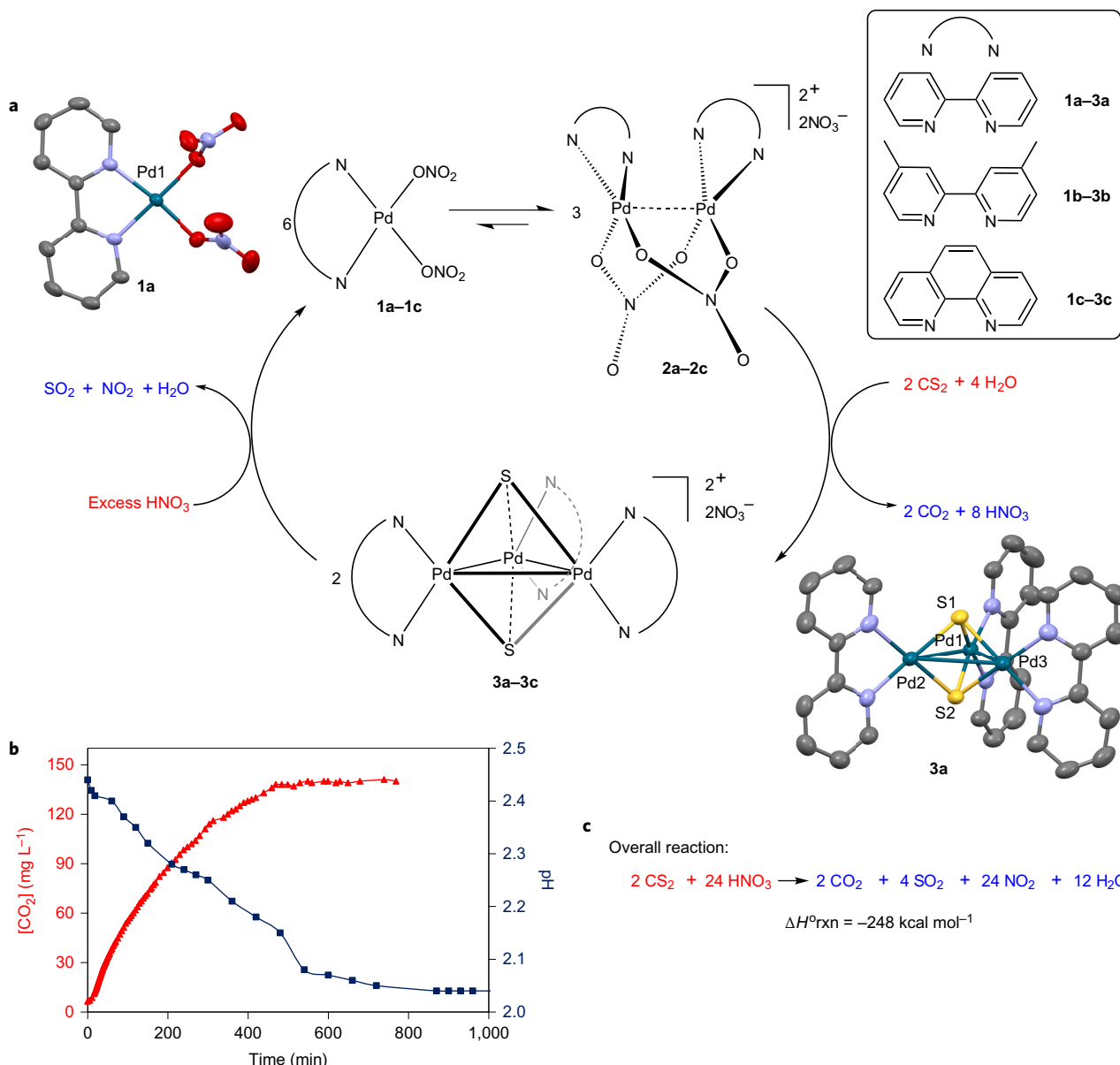


Figure 1 | Converting CS_2 into CO_2 using dimeric palladium complexes in water. **a**, Two sequential steps show the hydrolysis of CS_2 to generate CO_2 in the presence of aqueous $\text{2a-2NO}_3\text{-2c-2NO}_3$ to form $\text{3a-2NO}_3\text{-3c-2NO}_3$, and subsequent regeneration of $\text{2a-2NO}_3\text{-2c-2NO}_3$ with HNO_3 after the isolation of $\text{3a-2NO}_3\text{-3c-2NO}_3$. Attempts to make the reaction catalytic in $\text{HNO}_3(\text{aq})$ were not successful. The X-ray core structures of **1a** and **3a** are shown as ball-and-stick diagrams (hydrogen atoms (**1a** and **3a**) and PF_6^- anion (**3a**) are omitted for clarity). Selected bond lengths (\AA) and angles ($^\circ$) for **1a**, Pd1-O4, 2.040(3); Pd1-O1, 2.018(2); Pd1-N1, 1.987(3); Pd1-N2, 2.000(3); O4-Pd1-O1, 87.13(9); O4-Pd1-N2, 98.2(1); O1-Pd1-N1, 92.9(1); and for **3b**, Pd1-S1, 2.2618(7); Pd1-S2, 2.2825(7); Pd2-S1, 2.2912(8); Pd2-S2, 2.3045(9); Pd3-S1, 2.2898(8); Pd3-S2, 2.311(1); Pd1-S1-Pd, 90.72(2); Pd1-S1-Pd3, 89.80(2); Pd2-S1-Pd3, 77.05(2); P1-S2-Pd2, 98.86(2); Pd1-S2-Pd3, 88.75(2); Pd2-S2-Pd3, 76.37(2); S1-Pd2-S2, 76.06(2); S1-Pd1-S2, 77.07(2); S1-Pd3-S2, 75.95(2). **b**, $[\text{CO}_2]$ concentration and pH values versus time for the reaction of 2a-2NO_3 with CS_2 and H_2O at 22 °C. **c**, Reaction enthalpy for converting CS_2 and HNO_3 into CO_2 , NO_2 , SO_2 and H_2O . rxn, reactions.

Experimental characterization of reaction mechanism. Regarding the reaction pathway, the control reaction $\text{CS}_2 + \text{HNO}_3$ (dilute or concentrated) at 22 °C in water does not produce significant amounts of CO_2 , COS , NO_2 or SO_2 . Furthermore, a negative mercury-drop assay³² argues that Pd nanoparticles play no role in the double C–S cleavage process (see Supplementary Information). Stirring an aqueous solution of $[(\text{bpy})_2\text{Pd}_2(\text{NO}_3)_2](\text{NO}_3)_2$ (**2a-2NO₃**; bpy, 2,2'-bipyridine) with excess CS_2 at 22 °C for two hours quantitatively yields the trinuclear cluster $[(\text{bpy})_3\text{Pd}_3(\mu_3-\text{S})_2]^{2+}(\text{NO}_3)_2$ (**3a-2NO₃**), CO_2 and HNO_3 . The PF_6^- salt of **3a** is isolated in 94% yield by adding a tenfold excess of KPF_6 to aqueous **3a-2NO₃** (see Supplementary Information). Complex **3a-2PF₆** was characterized

by ^1H and ^{13}C NMR spectroscopy, electrospray ionization mass spectrometry (ESI-MS), elemental analysis and single-crystal X-ray diffraction. The ^1H NMR spectrum exhibits downfield signals at $\delta = 8.95 \sim 7.78$ ppm assignable to coordinated bpy ligands in a symmetrical environment, and the ^{13}C NMR exhibits five signals at $\delta = 155.47$, 151.04, 140.76, 127.61 and 123.79 ppm, which correspond to the five bpy ring carbon nuclei (Supplementary Fig. 2). Furthermore, the formation of **3a**²⁺ is supported by the ESI-MS feature at the mass-to-charge ratio (m/z) of 425.56 (Supplementary Fig. 3). The quasi- D_{3h} **3a-2PF₆** structure was confirmed by X-ray diffraction (Fig. 1a), and features a triangular M_3 core³³. In the distorted trigonal

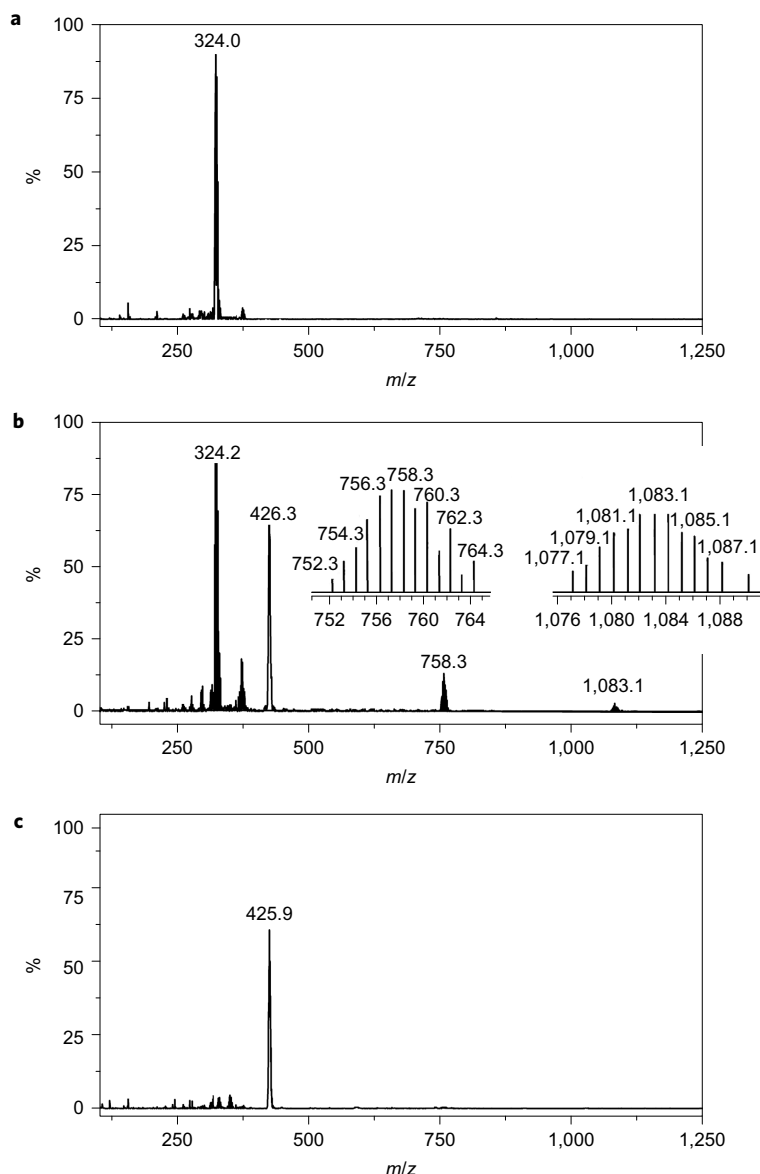


Figure 2 | Monitoring the reaction of CS_2 with 0.05 M aqueous $\mathbf{2a}\cdot\mathbf{2NO}_3$ by ESI-MS as a function of time. Both **4** and **10** are observed over the course of the reaction. The m/z peaks at 324.0 and 425.9 correspond to $[\mathbf{2a}\cdot\mathbf{NO}_3]^+$ and $[\mathbf{3a}]^{2+}$, respectively. **a**, $t = 0$ min. **b**, $t = 8$ min. **c**, $t = 35$ min.

bipyramidal Pd_3S_2 framework, all the Pd atoms are coordinated to a bpy ligand and bridged by two $\mu_3\text{-S}^{2-}$ ligands to form a Pd_3 isosceles triangle with two long edges and one short edge. The Pd-Pd distances Pd1...Pd2, Pd2...Pd3 and Pd3...Pd1 are 3.2396(5), 2.8535(7) and 3.2128(6) Å, respectively, which indicates relatively weak metal–metal interactions. The angles Pd1–Pd2–Pd3, Pd2–Pd1–Pd3 and Pd1–Pd3–Pd2 are 63.27(1)°, 52.49(1)° and 64.24(1)°, respectively. Neighbouring bpy units stack in an almost parallel manner with centroid–centroid distances of 4.62(8) and 4.48(2) Å for pyridyl pairs, which suggests weak intermolecular $\pi\cdots\pi$ interactions^{30,31,34–36}.

Regarding the transformation shown in Fig. 1c, the yield of CO_2 generated by the $\mathbf{2a}\cdot\mathbf{2NO}_3$ -mediated hydrolysis of the CS_2 C–S bonds is 57% within five minutes (Supplementary Information). The aqueous CO_2 concentration was monitored with a CO_2 -sensitive electrode and, as shown in Fig. 1b, the CO_2 concentration increases as the reaction proceeds until aqueous/dissolved and gaseous CO_2 reach equilibrium in the closed vessel. A molecular peak at m/z 44 in the gas-phase MS supports CO_2 generation. To confirm that CS_2 hydrolysis is the origin of the CO_2 , experiments were carried out with $^{13}\text{CS}_2$ and H_2^{18}O (Supplementary Figs 11–13). A molecular

ion at m/z 45 that corresponds to $^{13}\text{CO}_2$ is observed by MS for the reaction of $\mathbf{2a}\cdot\mathbf{2NO}_3$ with $^{13}\text{CS}_2$ and H_2O , which indicates the CO_2 is generated from CS_2 . Furthermore, $^{13}\text{C}^{18}\text{O}_2$ (m/z 49) is also observed when $\mathbf{2a}\cdot\mathbf{2NO}_3$ is reacted with $^{13}\text{CS}_2$ and H_2^{18}O , which confirms that the CO_2 oxygen originates from the H_2O . Consistent with the stoichiometry in Fig. 1b, the reaction mixture pH continuously falls as the reaction progresses, indicative of HNO_3 generation.

To probe further the mechanism of CS_2 hydrolysis, the reaction of an aqueous $\mathbf{2a}\cdot\mathbf{2NO}_3$ solution with CS_2 was monitored by Fourier-transform infrared spectroscopy (FTIR), gas-phase MS and on-line ESI-MS. Three days after a methanolic CS_2 solution was added to aqueous $\mathbf{2a}\cdot\mathbf{2NO}_3$ it exhibited strong absorption features in the FTIR spectrum at 2,350 and 666 cm^{-1} , which corresponds to CO_2 (refs 37,38), along with a strong CS_2 mode at 1,530 cm^{-1} and signals at 2,070 and 2,050 cm^{-1} attributable to COS (Supplementary Fig. 14)³⁸, implicating COS as a reaction intermediate or by-product^{37,38}. After ten days, the disappearance of the COS and CS_2 peaks is accompanied by growth of the CO_2 signal intensity, which suggests that COS is formed in the reaction, but is then consumed by reaction with $\mathbf{2a}\cdot\mathbf{2NO}_3$ to yield CO_2 .

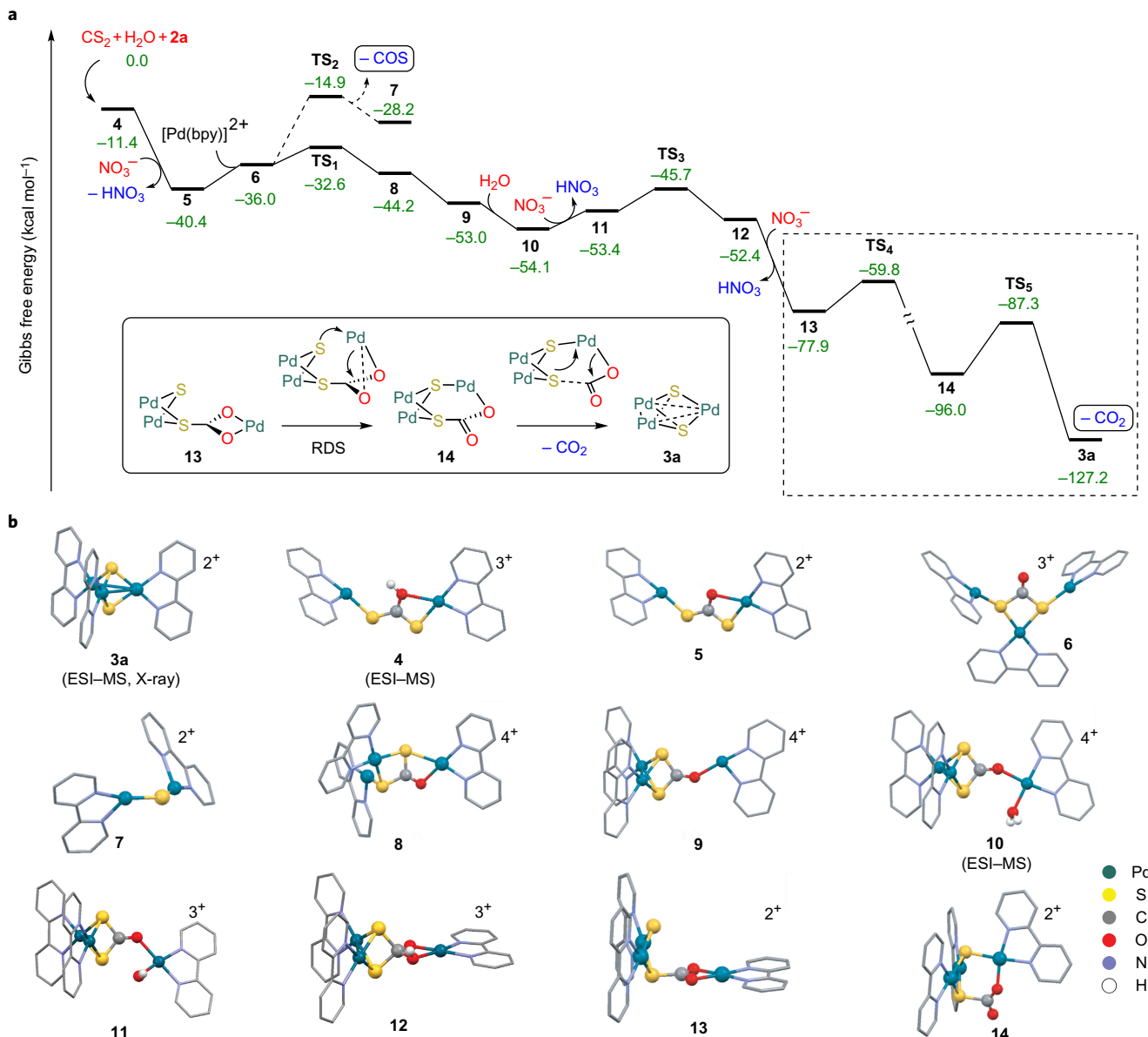


Figure 3 | Proposed mechanism for the reaction of 2a²⁺ with CS₂ from DFT calculations. **a**, DFT-computed pathway for the reaction of 2a²⁺ with CS₂. Computed relative free energies (kcal mol⁻¹) are given in green. **b**, DFT optimized molecular structures for the compounds in **a**. Selected hydrogen atoms removed for clarity.

The same reaction of an aqueous solution of 2a·2NO₃ with CS₂ was also investigated by gas-phase MS and on-line ESI-MS. The former exhibits a minor ion at *m/z* 60, which confirms the presence of COS (Supplementary Fig. 11) as a reaction product. Analysis by ESI-MS before CS₂ addition reveals an ion at *m/z* 324, corresponding to 2a·2NO₃ (Fig. 2a). On CS₂ addition, low-intensity features at *m/z* 1,083.9 and 758.9 were observed after eight minutes and are assignable to fragmentation ions (((bpy)Pd)₃(μ-OCS₂)(H₂O))(NO₃)₃⁺ and (((bpy)Pd)₂(μ-HOCS₂)(H₂O))(NO₃)₂⁺, respectively (Fig. 2b). After 35 minutes these peaks are absent, whereas the signal of the final product (((bpy)Pd)₃(μ³-S)²⁺ is detected at *m/z* 425.3 (Fig. 2c). Next, the independent reaction of COS in methanol with an aqueous 2a·2NO₃ solution was monitored by on-line ESI-MS. An ion at *m/z* 742 is observed, assignable to the (((bpy)Pd)₂(OCSOH)₂(NO₃)⁺ fragment of (((bpy)Pd)₃(OCSOH)₂)(NO₃)₄ (Supplementary Fig. 1). Furthermore, the reaction of 2a with COS produces 3a·2NO₃ and CO₂, the identities of which were confirmed by single-crystal X-ray diffraction and MS, respectively.

Finally, clusters 3a·2NO₃–3c·2NO₃ were treated with concentrated HNO₃ to yield the corresponding complexes 1a–1c, SO₂ and NO₂. The latter gases were confirmed by strong absorption peaks at 2,900 and 1,610 cm⁻¹ in the FTIR analysis (Supplementary Fig. 25), and an MS ion peak at *m/z* 46 (ref. 35). In addition to a gas-phase MS signal at *m/z* 64, assignable to SO₂, treating the solution with BaCl₂ yields a white solid, identified as BaSO₄ by FTIR and powder X-ray diffraction (Supplementary Figs 26 and 27)^{28,29} confirming SO₂ generation by HNO₃ oxidation of the Pd₃S₂ clusters. The structure of the mononuclear square-planar Pd complex 1a (Fig. 1a) was verified by single-crystal X-ray diffraction (Supplementary Fig. 30)³⁹. Recrystallization of 1a from water regenerates the active dimer 2a, also verified by X-ray diffraction, and verifies that 1a and 2a are in equilibrium. The position of the monomer–dimer equilibrium mainly depends on the concentration of NO₃⁻ (the monomeric structure is favoured at high NO₃⁻ concentrations and the dimeric structure at low NO₃⁻ concentrations) and the pH values (the monomer is favoured

in the strong acid solution). Regenerated monomeric complexes **1a–1c** again mediate C–S bond cleavage in CS₂ to form clusters **3a**·2NO₃·3c·2NO₃, presumably via dimeric **2a**·2NO₃·2c·2NO₃. Interestingly, both NO₂ (*m/z* 46) and SO₂ (*m/z* 64) are detected throughout the reaction of aqueous **2a** with CS₂ (Supplementary Figs 11 and 13), which indicates that the small amounts of HNO₃ formed throughout the reaction oxidize the Pd₃S₂ (**3a**) clusters *in situ*, consistent with slow catalytic turnover.

Computational analysis of CS₂ cleavage by dimeric Pd complexes. Based on the intermediates observed experimentally (see above), density functional theory (DFT) calculations were performed to probe the unusual hydrolysis mechanism of CS₂ mediated by **2a**·2NO₃ (Fig. 3 and Supplementary Information). From evidence that NO₃[−] does not coordinate to the Pd metal centre in the X-ray structure of the final product **3a**, we suppose that the NO₃[−] weakly coordinates to the Pd(II) metal centre in the reaction and readily dissociates from the intermediate Pd complexes. Furthermore, the intermediates generated from CS₂ hydrolysis, such as S₂C=OH[−], S₂C=O₂[−], SOC=OH[−] and SOC=O₂[−], may coordinate more strongly to Pd ions in chelating and bridging modes than does NO₃[−] during the process of the CS₂ and COS hydrolysis. Therefore, the coordinative interactions and energy influence from all NO₃[−] counterions in the DFT calculations are omitted during the reaction. With the NO₃[−] counteranions thus omitted, computation begins from $\text{[(bpy)Pd]}_2(\mu\text{-HOCS}_2)(\text{H}_2\text{O})^{2+}$ (**4**) because this dithiocarbonate is observed by ESI-MS. Species **4** is readily deprotonated to yield **5**, and reacts with a [(bpy)Pd]^{2+} fragment to form trimer **6**, and the subsequent exoergic (−17 kcal mol^{−1}) rearrangement of **6** to **9** occurs in two steps. First, an H₂O molecule binds to the open Pd coordination site, which also coordinates the oxygen of the bound OCS₂^{2−} fragment in $\text{[(bpy)Pd]}_3(\mu\text{-OCS}_2)(\text{H}_2\text{O})^{4+}(\text{NO}_3)_3^+$ (**10**), observed by ESI-MS. The coordinated water molecule is subsequently deprotonated by NO₃[−] to yield a Pd-OH moiety (**11**). This nucleophilic Pd-OH moiety⁴⁰ intramolecularly attacks the μ-OCS₂ C atom to produce complex **12**. On deprotonation, one C–S bond is broken to form complex **13**. This is followed by the rate-determining Pd–O bond cleavage and Pd–S bond formation to yield complex **14** with a barrier of +18.1 kcal mol^{−1}. The final exoergic (−31.2 kcal mol^{−1}) step involves simultaneous C–S bond cleavage and CO₂ release to afford the trimetallic complex **3a**²⁺ (Fig. 3). In the process of CS₂ hydrolysis, COS can be formed as a by-product from **6** via transition state TS₂ with a barrier of +21.1 kcal mol^{−1}. This slightly higher barrier than that of the rate-limiting step from **13** to **14** is consistent with the minor amounts of COS observed. Overall, the computed steps in the proposed mechanism (Fig. 3) are found to be both kinetically and thermodynamically accessible at 25 °C.

To explore the scope of dimeric Pd complexes competent for CS₂ cleavage, Pd₂ complexes $[(\text{dm bpy})\text{Pd}_2](\text{NO}_3)_4$ (**2b**·2NO₃) (ref. 41) and $[(\text{phen})\text{Pd}_2](\text{NO}_3)_4$ (**2c**·2NO₃) (ref. 42) (dm bpy, 4,4'-dimethylbipyridine; phen, 1,10-phenanthroline) were also investigated for CS₂ cleavage in aqueous solution. Significantly, the results of ESI-MS, pH changes, [CO₂(aq)] assay and single-crystal X-ray diffraction show that both C–S bonds of CS₂ are cleaved by **2b**·2NO₃ and **2c**·2NO₃ at 25 °C to generate CO₂ and the Pd₃S₂ clusters **3b**·2NO₃ and **3c**·2NO₃ (Supplementary Figs 15–20 and 31). Not surprisingly, Pd intermediates similar to species **9** derived from **2a**·2NO₃ are detected by on-line ESI-MS as signals at *m/z* 1,165.5 and 1,155.5, which correspond to $\text{[(dm bpy)Pd]}_3(\mu\text{-OCS}_2)(\text{H}_2\text{O})^{+}(\text{NO}_3)_3^+$ (Supplementary Fig. 15) and $\text{[(phen)Pd]}_3(\mu\text{-OCS}_2)(\text{H}_2\text{O})^{+}(\text{NO}_3)_3^+$ (Supplementary Fig. 16), respectively. These are observed in the reactions that involve **2b**·2NO₃ and **2c**·2NO₃, and this argues that Pd complexes with different ancillary ligands operate via a mechanism similar to that of **2a**·2NO₃.

Conclusions

It is shown here that air- and moisture-tolerant dimeric Pd₂ complexes quantitatively cleave the C–S bonds of CS₂ in aqueous solution to yield Pd₃(μ₃-S)₂ clusters. The complexes can be regenerated fully with strong oxidants at room temperature to complete the elements of a catalytic cycle. To our knowledge, this is the first process to cleave both C–S bonds under ambient conditions, and opens new possibilities for neutralizing CS₂ and COS pollutants.

Received 23 February 2016; accepted 5 September 2016;
published online 24 October 2016

References

- Topsoe, H. *et al.* The role of reaction pathways and support interactions in the development of high activity hydrotreating catalysts. *Catal. Today* **107**–**108**, 12–22 (2005).
- Wang, L., He, W. & Yu, Z. Transition-metal mediated carbon–sulfur bond activation and transformations. *Chem. Soc. Rev.* **42**, 599–621 (2013).
- Gary, J. H., Handwerk, G. E. & Kaiser, M. J. *Petroleum Refining: Technology and Economics* (CRC, 2007).
- Stavtsov, A. K., Drozdovskii, V. N., Irklei, V. M., Mokrousova, L. A. & Napalkova, T. A. Effect of carbon disulfide consumption on the basic properties of viscose prepared from radiation-modified cellulose. *Fibre Chem.* **23**, 396–399 (1992).
- Notholt, J. *et al.* Enhanced upper tropical tropospheric COS: impact on the stratospheric aerosol layer. *Science* **300**, 307–310 (2003).
- Sze, N. D. & Ko, M. K. W. CS₂ and COS in the stratospheric sulphur budget. *Nature* **280**, 308–310 (1979).
- Sze, N. D. & Ko, M. K. W. Is CS₂ a precursor for atmospheric COS? *Nature* **278**, 731–732 (1979).
- Turco, R. P., Whitten, R. C., Toon, O. B., Pollack, J. B. & Hamill, P. OCS, stratospheric aerosols and climate. *Nature* **283**, 283–285 (1980).
- Cox, R. A. & Sheppard, D. Reactions of OH radicals with gaseous sulphur compounds. *Nature* **284**, 330–331 (1980).
- Deshmukh, M. M., Ohba, M., Kitagawa, S. & Sakaki, S. Absorption of CO₂ and CS₂ into the Hofmann-type porous coordination polymer: electrostatic versus dispersion interactions. *J. Am. Chem. Soc.* **135**, 4840–4849 (2013).
- Wang, X. Q. *et al.* Adsorption of carbon disulfide on Cu/CoSPc/Ce modified activated carbon under microtherm and micro-oxygen conditions. *Ind. Eng. Chem. Res.* **53**, 13626–13634 (2014).
- Cullis, C. F. & Mulcahy, M. F. R. The kinetics of combustion of gaseous sulphur compounds. *Combust. Flame* **18**, 225–292 (1972).
- Laperdriz, E. *et al.* Comparative study of CS₂ hydrolysis catalyzed by alumina and titania. *Appl. Catal. B* **17**, 167–173 (1998).
- Mukherjee, S., Das, S. K. & Biswas, M. N. Absorption of carbon disulphide in alkaline solution in spray and ejector columns. *Chem. Eng. Process.* **46**, 181–186 (2007).
- Azatyar, V. V. The role of a reaction of direct substitution for a sulfur atom in the CS₂ molecule in the combustion of carbon disulfide with oxygen. *Kinet. Catal.* **44**, 459–462 (2003).
- Tong, S., Dalla Lana, I. G. & Chuang, K. T. Kinetic modeling of the hydrolysis of carbon disulfide catalyzed by either titania or alumina. *Can. J. Chem. Eng.* **73**, 220–227 (1995).
- Smeulders, M. J. *et al.* Evolution of a new enzyme for carbon disulphide conversion by an acidothermophilic archaeon. *Nature* **478**, 412–416 (2011).
- Wang, J. C., Zlotnick, A. & Mecinović, J. Transmission electron microscopy enables the reconstruction of the catenane and ring forms of CS₂ hydrolase. *Chem. Commun.* **50**, 10281–10283 (2014).
- Werner, H. Novel coordination compounds formed from CS₂ and heteroallenes. *Coord. Chem. Rev.* **43**, 165–185 (1982).
- Pandey, K. K. Reactivities of carbonyl sulfide (COS), carbon disulfide (CS₂) and carbon dioxide (CO₂) with transition metal complexes. *Coord. Chem. Rev.* **140**, 37–114 (1995).
- Ibers, J. A. Centenary Lecture. Reactivities of carbon disulphide, carbon dioxide, and carbonyl sulphide towards some transition-metal systems. *Chem. Soc. Rev.* **11**, 57–73 (1982).
- Lide, D. R. *CRC Handbook of Chemistry and Physics* (CRC, 2004).
- Johnson, A. R. *et al.* Four-coordinate molybdenum chalcogenide complexes relevant to nitrous oxide N–N bond cleavage by three-coordinate molybdenum (III): synthesis, characterization, reactivity, and thermochemistry. *J. Am. Chem. Soc.* **120**, 2071–2085 (1998).
- Ballmann, J. *et al.* Complete disassembly of carbon disulfide by a ditantalum complex. *Chem. Commun.* **46**, 8794–8796 (2010).
- Kallane, S. I. *et al.* Remarkable reactivity of a rhodium(I) boryl complex towards CO₂ and CS₂: isolation of a carbido complex. *Chem. Commun.* **51**, 14613–14616 (2015).
- Ariafard, A., Brookes, N. J., Stranger, R. & Yates, B. F. Activation of CS₂ and CS by ML₃ complexes. *J. Am. Chem. Soc.* **130**, 11928–11938 (2008).

27. Thiemann, M., Scheibler, E. & Wiegand, K. W. in *Ullmann's Encyclopedia of Industrial Chemistry* (Wiley-VCH, 2000); http://onlinelibrary.wiley.com/doi/10.1002/14356007.a17_293/full
28. Farrar, D. H., Gukathasan, R. R. & Morris, S. A. Reaction of carbon disulfide with trinuclear palladium and platinum clusters. Crystal structure of $\text{Pt}_2(\mu\text{-CS}_2)_2(\text{P}(t\text{-Bu})_2\text{Ph})_2$. *Inorg. Chem.* **23**, 3258–3261 (1984).
29. Kullberg, M. L. & Kubik, C. P. Insertions of small molecules, carbon monoxide, methyl isocyanide, sulfur dioxide, and carbon disulfide, into the Pd–Pd σ -bond of $\text{Pd}_2\text{Cl}_2(\text{PMe}_2\text{CH}_2\text{PMe}_2)_2$. Crystal and molecular structure of $\text{Pd}_2(\mu\text{-CO})\text{Cl}_2(\text{PMe}_2\text{CH}_2\text{PMe}_2)_2$. *Inorg. Chem.* **25**, 26–30 (1986).
30. Bradford, A. M., Jennings, M. C. & Puddephatt, R. J. Scope and mechanism of oxidative addition of carbon-sulfur double bonds to trinuclear platinum and palladium complexes. *Organometallics* **8**, 2367–2371 (1989).
31. Ingram, A. J., Solis-Ibarra, D., Zare, R. N. & Waymouth, R. M. Trinuclear Pd_3O_2 intermediate in aerobic oxidation catalysis. *Angew. Chem. Int. Ed.* **53**, 5648–5652 (2014).
32. Widegren, J. A. & Finke, R. G. A review of the problem of distinguishing true homogeneous catalysis from soluble or other metal-particle heterogeneous catalysis under reducing conditions. *J. Mol. Catal. A* **198**, 317–341 (2003).
33. Tzeng, B.-C. *et al.* Palladium(II) and platinum(II) analogues of luminescent diimine *Triangulo* complexes supported by triply bridging sulfide ligands: structural and spectroscopic comparisons. *Inorg. Chem.* **40**, 6699–6704 (2001).
34. Ingram, A. J., Walker, K. L., Zare, R. N. & Waymouth, R. M. Catalytic role of multinuclear palladium–oxygen intermediates in aerobic oxidation followed by hydrogen peroxide disproportionation. *J. Am. Chem. Soc.* **137**, 13632–13646 (2015).
35. Leoni, P. *et al.* Synthesis and structure of $\text{Pd}_4(\mu\text{-PtBu}_2)_2(\mu\text{-CS}_2)(\text{PPh}_3)_2\text{I}_2$, a neutral palladium(I) derivative with a hexacoordinate carbon and a CS_2 molecule bridging four palladium centers. *J. Am. Chem. Soc.* **119**, 8625–8629 (1997).
36. Tzeng, B.-C., Wu, Y.-L. & Kuo, J.-H. Supramolecular assembly of *Triangulo* Pd(II) diimine complexes containing triply-bridging sulfide ligands. *J. Chin. Chem. Soc.* **53**, 1033–1038 (2006).
37. Pugh, L., Rao, K. N. & Rao, K. N. in *Molecular Spectroscopy: Modern Research*, Vol. II (ed. Rao, K. N.) 165 (Academic, 1976).
38. Person, W. B., Brown, K. G., Steele, D. & Peters, D. *Ab initio* calculations of vibrational properties of some linear triatomic molecules. 1. Intensities. *J. Phys. Chem.* **85**, 1998–2007 (1981).
39. Adrian, R. A., Zhu, S., Klausmeyer, K. K. & Walmsley, J. A. Synthesis and X-ray crystal structure determination of monomeric *cis*-Pd(2,2'-bipyridine)(NO_3)₂. *Inorg. Chem. Commun.* **10**, 1527–1530 (2007).
40. Fulmer, G. R., Herndon, A. N., Kaminsky, W., Kemp, R. A. & Goldberg, K. I. Hydrogenolysis of palladium(II) hydroxide, phenoxide, and alkoxide complexes. *J. Am. Chem. Soc.* **133**, 17713–17726 (2011).
41. Yu, S.-Y. *et al.* Solution self-assembly, spontaneous deprotonation, and crystal structures of bipyrazolate-bridged metallocacycles with dimetal centers. *Inorg. Chem.* **44**, 9471–9488 (2005).
42. Tong, J., Yu, S.-Y. & Li, H. Programmable self-assembly of homo- or heterometallocacycles using 4-(1H-pyrazolyl-4-yl)pyridine. *Chem. Commun.* **48**, 5343–5345 (2012).

Acknowledgements

This research was supported by National Natural Science Foundation of China (Grant numbers 21471011, 21574135, 91127039, 51303180, 21203245, 21532005, 21327010), the Beijing Natural Science Foundation (Grant 2162043), the One Hundred Talents Program, the Chinese Academy of Sciences, the Importation and Development of High-Caliber Talents Project of the Beijing Municipal Institution and Beijing Postdoctoral Research Foundation (Grant 2015M570017) and the Beijing Synchrotron Radiation Facility for crystal structure determination using synchrotron radiation X-ray diffraction analysis. We also thank H. Ma (Beijing Institute of Technology) for the X-ray crystallography. Research at Northwestern University is supported by the US National Science Foundation under grant CHE-1464488. The Northwestern CleanCat Core Facility acknowledges funding from the US Department of Energy (Grant DE-FG02-03ER15457) used for the purchase of the portable universal gas analyser. We thank N. M. Schweitzer for supporting the mass spectroscopy.

Author contributions

S.-Y.Y. and H.H. conceived the study. H.H., S.-Y.Y., M.D., T.L.L. and T.J. M. planned the research. X.-F.J., H.H. and T.L.L. synthesized and characterized the compounds. Y.-J.P. and Y.-F.C. conducted the on-line ESI experiments and analysis. W.L. conducted the DFT calculations. H.H., X.-F.J., T.L.L., S.-Y.Y., W.L., M.D. and T.J.M. prepared the manuscript. All the authors commented on the manuscript.

Additional information

Supplementary information and chemical compound information are available in the [online version of the paper](#). Reprints and permissions information is available online at www.nature.com/reprints. Correspondence and requests for materials should be addressed to H.H., S.-Y.Y., W.L., Y.-J.P., M.D. and T.J.M.

Competing financial interests

The authors declare no competing financial interests.